Implications of Supramolecular Crosslinking on Hydrogel Toughening by Directional Freeze-Casting and Salting-Out

Zhou Ye,[1] Teng Chi,[1] Connor J. Evans,[2] Dongping Liu,[1] Christopher J. Addonizio,[1] Bo Su,[1] Irawan Pramuyda,[1] Yuanhui Xiang,[1] Ryan K. Roeder,[2,3,4] Matthew J. Webber[1,3,4]*

[1] Department of Chemical & Biomolecular Engineering
[2] Department of Aerospace and Mechanical Engineering
[3] Bioengineering Graduate Program
[4] Materials Science and Engineering Graduate Program
University of Notre Dame
Notre Dame, IN 46556, USA
E-mail: mwebber@nd.edu

Supporting information for this article is given via a link at the end of the document.

Abstract: Dynamic hydrogel crosslinking captures network reorganization and self-healing of natural materials, yet is often accompanied by reduced mechanical properties compared to covalent analogues. Toughening is possible in certain materials with processing by directional freeze-casting and salting-out, producing hierarchically organized networks with enhanced mechanical properties. The implications of including dynamic supramolecular crosslinking alongside such processes are unclear. Here, a supramolecular hydrogel prepared from homoternary crosslinking by pendant guests with a free macrocycle is subsequently processed by directional freeze-casting and salting-out. The resulting hydrogels tolerate multiple cycles of compression. Excitingly, supramolecular affinity dictates the mechanical properties of the bulk hydrogels, with higher affinity interactions producing materials with higher Young's modulus and enhanced toughness under compression. The importance of supramolecular crosslinking is emphasized with a supramolecular complex that is converted *in situ* into a covalent crosslink. While supramolecular hydrogels do not fracture and spontaneously self-heal when cut, their covalent analogues fracture under moderate strain and do not self-heal. This work shows a molecular-scale origin of bulk hydrogel toughening attributed to affinity and dynamics of supramolecular crosslinking, offering synergy in combination with post-processing techniques to yield materials with enhanced mechanical properties tunable at the molecular scale for the needs of specific applications.

Introduction

The development of tough hydrogels with dynamic and self-healing properties has been an area of focus in recent years, with potential applications in diverse fields of tissue engineering,[1,2] soft robotics,[3] and wearable electronics.[4] Several strategies have been reported to prepare tough hydrogels by introducing anisotropy in the underlying polymer architecture, including through muscle-inspired mechanical training,[5,6] or directional freeze-casting and salting-out.[7] Directional freeze-casting, also known as ice-templating, is a versatile technique that endows polymeric hydrogels with aligned and hierarchical architecture by controlling the rate and direction of freezing, resulting in materials with aligned organization reminiscent of that found in natural load-bearing tissues and significantly enhanced mechanical properties.[8–10] The salting-out effect, meanwhile, is a well-known phenomenon in polymer science that arises by precipitation of polymers from an aqueous solution upon the addition of salts.[11,12] In the context of hydrogel fabrication, salting-out can promote the formation of nanofibers and other structures in the hydrogel, leading to improved mechanical properties and toughness through enhanced chain bundling.[7]

A variety of strategies have been explored to engineer hydrogels with dynamic mechanical properties and self-healing character.[13,14] Among the different types of dynamic interactions that can govern dynamic properties on the bulk scale,[15] supramolecular recognition offers a useful design approach to take advantage of reversible and equilibrium-governed molecular-scale interactions in constructing materials.[16,17] Of the various supramolecular interactions used, host–guest recognition and crosslinking offers a particularly useful approach to design and tune dynamic and reversible hydrogel network junctions.[18,19] The cucurbit[n]uril (CB[n]) family of macrocycles affords affinity to a broad array of guests;[20] a member of this family, CB[8], simultaneously binds two guests within its portal.[21] Accordingly, the display of guests pendant from polymer building blocks enables addition of free CB[8] to form ternary complex crosslinks, with approaches using either two identical (homoternary)[22] or complementary and/or cooperative (heteroternary)[23] guests as crosslinking interactions. Heteroternary CB[8]–guest crosslinking with slow exchange dynamics was recently shown to yield networks with tough, glass-like character that still retain self-healing properties.[24] At the same time, supramolecular hydrogels often have relatively weak mechanical properties and limited toughness, as the dynamic nature of their underlying non-covalent interactions can be at odds with mechanical strength and lead to flow under application of moderate strain.[16] Indeed, strategies to enhance the mechanical properties of supramolecular hydrogels are an active area of research in order to harness the otherwise appealing properties of this class of dynamic soft materials.[25] In this way, integrating post-processing techniques like directional freeze-casting and salting-out offer an appealing approach in order to introduce hierarchical anisotropy and structural ordering for the purpose of creating tough supramolecular hydrogels.

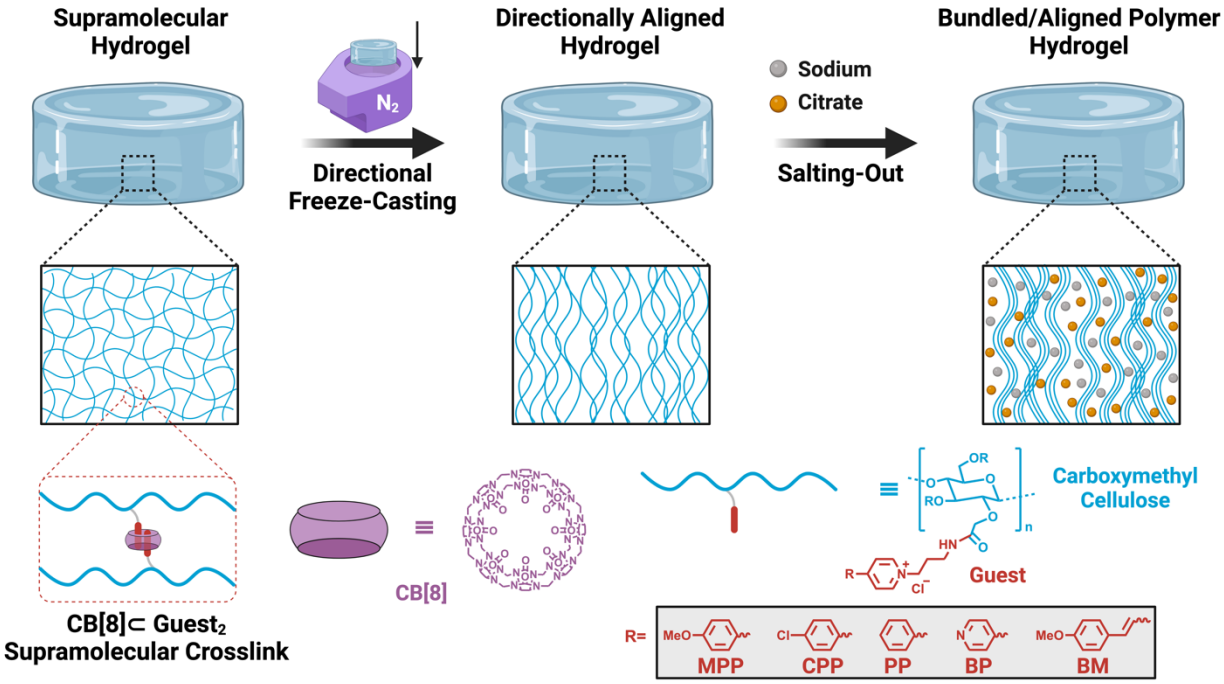

Figure 1: Schematic overview of the approach to enable hierarchical organization of supramolecular hydrogels through post-processing steps of directional freeze-casting and salting-out (*top*). Of particular interest in the study here is the use of dynamic supramolecular crosslinking (*bottom*) between carboxymethylcellulose (CMC) with pendant guests that form a 2:1 ternary complex with free cucurbit[8]uril (CB[8]). The guest chemistry can be varied to control the affinity, and concomitant dynamics, of the supramolecular interaction as shown in the molecular structure overview.

Here, a method is reported to prepare tough and self-healing hydrogels with multiscale control by combining supramolecular host–guest recognition and crosslinking having tunable affinity and concomitant dynamics with directional freeze-casting and salting-out (***Fig 1***). Though these processing steps have a history of use in hydrogel toughening, the implications of their use in conjunction with dynamic supramolecular crosslinking for hydrogel toughening are less known. At the molecular-scale, a carboxymethyl cellulose (CMC) backbone is modified by guests with tunable homoternary affinity for a free CB[8] macrocycle. On the nano- to micro-scales, directional freeze-casting affords an anisotropic network architecture aligned in the direction of freezing, with subsequent salting-out stiffening and bundling the aligned polymer filaments. This approach to hydrogel design and processing integrates the dynamics of a supramolecular network alongside hierarchical organization from post-processing with directional freeze-casting and salting-out, resulting in a biomimetic material that exhibits directional toughness and self-healing capabilities that are tunable according to the underlying supramolecular interactions.

Results and Discussion

Synthesis of Guest-Modified CMC. Carboxymethyl cellulose (CMC) was modified to present guests with a conserved pyridinium core structure that was para-modified with four R-groups (***Fig 1***): 4-methoxy phenyl (**MPP**), 4-chloride phenyl (**CPP**), phenyl (**PP**), and pyridine (**BP**). These designs were intended to tailor the electronic properties of the guest molecules, informed by studies detailing the importance of aromatic electronics on CB[8]–guest ternary complex dynamics.[24] The methoxy group is typically electron donating in the π-direction, while the chlorine is a weak electron donor in π-direction but strongly withdraws electrons in the *σ*-direction.[26] The pyridine and phenyl groups were likewise selected for their respective electron-withdrawing/donating abilities. Guests bearing these groups were synthesized by first attaching these R-groups to a core pyridinium structure in its para position via Suzuki couplings, and subsequently reacting the pyridine moiety with 3-Chloropropylamine to yield the four guests for CMC modification (***Scheme S1***): 1-(3-aminopropyl)-4-(4-methoxyphenyl)pyridin-1-ium chloride , 1-(3-aminopropyl)-4-(4-chlorophenyl)pyridin-1-ium chloride, 1-(3-aminopropyl)-4-phenylpyridin-1-ium chloride, and 1-(3-aminopropyl)-[4,4'-bipyridin]-1-ium chloride, as detailed in the online supporting information. All guests were fully characterized by ^{1}H NMR (***Fig S1-S5***). CMC of 90 kDa molecular weight was then modified through coupling the amines on each guest to its carboxylates with 4-(4,6-Dimethoxy-1,3,5-triazin-2-yl)-4-methylmorpholinum chloride (DMTMM). A degree of substitution of 6.5-7.0% was obtained

from ^{1}H NMR analysis (***Fig S13-S16***). To enable studies exploring the impact of CMC molecular weight, both 250 kDa and 700 kDa CMC were also modified with MPP and BP guests (***Fig S18-S21***). To enable studies on the importance of supramolecular crosslinking on mechanical properties, CMC was also modified with a Brooker's merocyanine (**BM**) guest (***Fig 1, Fig S17***). The choice of this guest stemmed from its similar structure to the MPP guest, but BM has a double bond for subsequent *in situ* conversion of the supramolecular crosslinking interactions into covalent crosslinking by a [2+2] photodimerization reaction catalyzed by CB[8] ternary complexation.[22,27] The synthesis of the BM guest was analogous to the other guests, with an additional step of a base-catalyzed condensation reaction (***Scheme S1, Fig S10-S11***).

CB[8]–Guest Recognition. CB[8] binding to each of the guest-modified CMCs was supported by upfield shifting and broadening of aromatic protons when measured by ^{1}H NMR (***Fig S22-S25***). In order to quantitatively characterize CB[8]–guest binding, isothermal titration calorimetry (ITC) was performed. Model guests were synthesized by reacting the four small molecule guests used for conjugation to CMC with acetic anhydride in order to recreate the form of the amide-linked guest when it is presented on CMC and eliminate any contributions from the terminal amino group on binding affinity (***Fig S6-S9***). The resulting small molecule guests (PP-Ac, MPP-Ac, CPP-Ac, and BP-Ac) were then assessed by ITC for their stoichiometry and thermodynamics of binding to CB[8] as a homoternary complex. A solution of the ligand in water was titrated into CB[8] in water. Each system underwent three independent experiments, and the heats of injection were fit with global analysis using a sequential binding model (A+B+B ↔ AB+B ↔ABB).[28] The experiments yielded overall binding constants, K_{eq} (M^{-2}), of the ternary complex with observed affinity for the first (K_1, M^{-1}) and second (K_2, M^{-1}) binding event (***Table 1, Fig S27***). From these data, the cooperativity factor α (α = K_2/K_1) was also calculated. A general trend in overall binding affinity of PP > MPP ≈ CPP > BP was observed from ITC. These general trends in affinity are in agreement with a prior report evaluating ternary CB[8]–guest affinity for a closely related series of guests.[26] These trends furthermore conform to expectations on the basis of molecular design. The phenyl group (PP) maintains a state of relative neutrality, situated between electron withdrawal and donation, without additional electron pairs or charges that could cause repulsion with the pyridinium units upon ternary complex formation. Both the methoxy (MPP) and chloride (CPP) groups have lone pair electrons that may interact with the second guest, exerting relatively similar effects in both π and σ directions, thereby explaining the comparable binding affinities of these two guests. Pyridine (BP) acts as an electron-withdrawing group, and when combined with the positive charge from the pyridinium may alter the polarity and hydrophobicity of the molecule, thereby leading to a relatively lower binding affinity; this guest may further introduce electrostatic repulsion when arranged in an antiparallel configuration in the ternary complex. The control molecule, BM, had an affinity of the same order as MPP and CPP. On the basis of cooperativity, values of α < 0.5 for homoternary complexes are typically characterized as having negative cooperativity, while values of 1 > α > 0.5 are typically characterized as being non-cooperative and values of α > 1 are cooperative.[29,30] MPP was the only molecule exhibiting non-cooperativity (α = 0.5) while all other guests had negative cooperativity. Thus, in all cases the binding of the first molecule tended to inhibit the binding of the second molecule as they arranged themselves in an expected antiparallel assembly within the CB[8] cavity to maximize distance between the constitutive positive charges of their pyridinium groups.

Table 1: Results from ITC experiments on model guests binding to CB[8]. Data obtained from a model of A+B+B ↔ AB + B ↔ ABB using a global fitting method on multiple replicate experiments (*n=3/guest*)

Guest	K_{eq} (M^{-2})	K_1 (M^{-1})	K_2 (M^{-1})	α
PP-Ac	$(4.48\pm0.68)\times10^{14}$	2.36×10^{8}	1.90×10^{6}	8.04×10^{-3}
MPP-Ac	$(3.14\pm0.85)\times10^{13}$	7.89×10^{6}	5.04×10^{6}	5.04×10^{-1}
CPP-Ac	$(2.90\pm0.08)\times10^{13}$	1.80×10^{7}	1.61×10^{6}	8.95×10^{-2}
BP-Ac	$(2.68\pm0.05)\times10^{12}$	7.88×10^{6}	3.40×10^{6}	4.32×10^{-2}
BM-Ac	$(1.40\pm2.06)\times10^{13}$	1.13×10^{7}	1.23×10^{6}	1.09×10^{-1}

Supramolecular Hydrogel Formation. CB[8]–guest supramolecular hydrogels were formed by mixing guest-modified CMC with CB[8] at a 2:1 ratio of guest to CB[8] and a total material concentration of 5% w/v in water. The mechanical properties of these hydrogels were evaluated using dynamic oscillatory rheology. Frequency sweep rheological analysis offers a means of studying the dynamics and network topology of supramolecular hydrogels.[15,19] When measured at 25°C (***Fig 2a***), CMC-MPP⊂CB[8], CMC-CPP⊂CB[8], and CMC-PP⊂CB[8] hydrogels had nearly identical behavior, including comparable plateau G' values and critical frequencies (ω_c, G' = G") that occurred near 0.1 rad/s and indicated very slow exchange dynamics of CB[8]–guest crosslinking in the networks. By comparison, CMC-BP⊂CB[8] hydrogels were significantly more dynamic and though a plateau G' value was not recorded within the frequency limits of the experiment the network exhibited characteristics of a reduced extent of network crosslinking (lower G'). Given the slow network exchange dynamics, experiments were also performed at 55°C, intended to accelerate network dynamics and better visualize differences between the different crosslinking chemistries (***Fig 2b***). At elevated temperatures, ω_c could be measured for the less dynamic networks, revealing a trend in network dynamics of

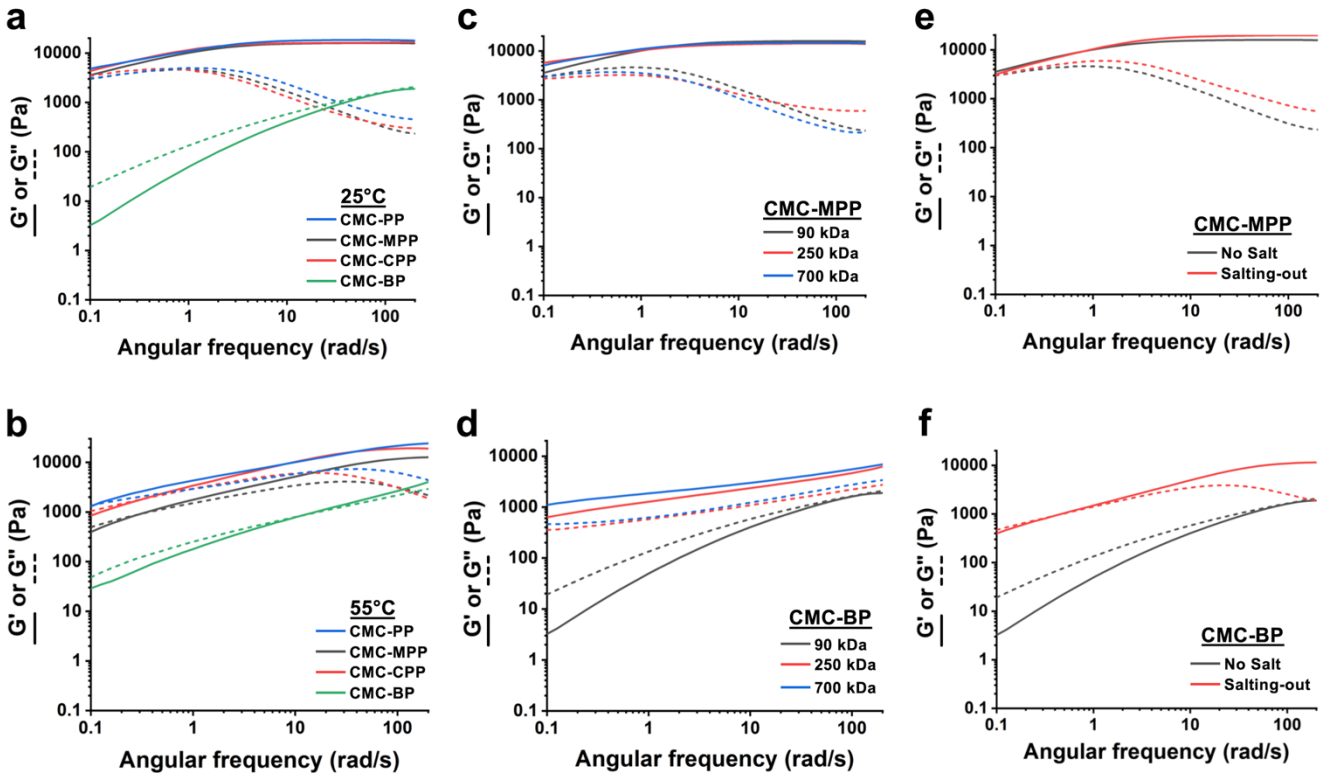

Figure 2: Dynamic oscillatory rheology on CMC-Guest⊂CB[8] supramolecular hydrogels prepared in DI water at 5% (w/v) in all cases. (**a**) Frequency sweep of different guest chemistries appended to 90 kDa CMC and compared at 25°C and (**b**) 50 °C on the basis of their storage modulus (G', solid lines) and loss modulus (G'', dashed lines). The impact of CMC molecular weight was the probed using frequency sweeps on guest chemistries of (**c**) MPP and (**d**) BP appended to 90 kDa, 250 kDa, and 700 kDa CMC. Finally, the impact of adding 1.5 M sodium citrate as done during salting-out processing, was assessed by frequency sweeps on hydrogels prepared from 90 kDa CMC with guest chemistries of (**e**) MPP and (**f**) BP.

CMC-PP⊂CB[8] (ω_c = 0.1 rad/s) < CMC-MPP⊂CB[8] (ω_c = 0.32 rad/s) ≈ CMC-CPP⊂CB[8] (ω_c = 0.32 rad/s) < CMC-BP⊂CB[8] (ω_c = 12.6 rad/s). As such the least dynamic network corresponded to the guest chemistry (PP) with the highest measured affinity by ITC, while the most dynamic network came from the lowest affinity CB[8]–guest interaction (BP).

One network with intermediate dynamics, CMC-MPP⊂CB[8], and the most dynamic network, CMC-BP⊂CB[8], were selected to study the effects of CMC molecular weight on the dynamics of hydrogels prepared at 5% w/v. For CMC-MPP⊂CB[8] hydrogels (***Fig 2c***), differences in both ω_c and plateau G' were negligible across CMC molecular weights ranging from 90-700 kDa. However, for the highly dynamic CMC-BP⊂CB[8] networks (***Fig 2d***), significant differences were observed between CMC of 90 kDa and the other molecular weights of 250 kDa and 700 kDa, with 90 kDa exhibiting higher dynamics and reduced mechanical properties. This points to added contribution for CMC chain entanglements in the presence of lower affinity and more dynamic CB[8]–guest crosslinking that were largely negligible in hydrogels prepared from higher affinity CB[8]–guest crosslinking.

Next, the impact of exposure to salting-out conditions was probed by assessing network dynamics when prepared at 1.5 M sodium citrate. The addition of sodium citrate at this high concentration is known to induce the formation of nanoscale bundling and aggregation in CMC.[31] When comparing rheological properties of CMC-MPP⊂CB[8] and CMC-BP⊂CB[8] with and without salts using 90 kDa CMC polymer, it was found that salting-out had negligible impact on the dynamics or mechanical properties of the less dynamic and more mechanically robust CMC-MPP⊂CB[8] network (***Fig 2e***), while salt significantly increased G' and simultaneously reduced the network dynamics of the CMC-BP⊂CB[8] network (***Fig 2f***). This again points to greater contributions from CMC chain entanglements when using lower affinity and more dynamic CB[8]–guest crosslinking.

Directional Freeze-Casting and Salting-Out. Supramolecular CMC-guest⊂CB[8] hydrogels were prepared in glass vials by dissolving the components at a total concentration of 5% w/v in water and then subjecting these to directional freeze-casting in liquid nitrogen through a home-

built apparatus to control the rate and direction of freezing (***Movie S1***). The frozen hydrogels were immediately transferred to 1.5 M sodium citrate for 24 h to initiate the salting-out process. Interestingly, without initial supramolecular crosslinking to form hydrogels, the materials dissolved during the salting-out processing step (***Movie S2***). The synergistic toughening effect of directional freeze-casting and salting-out of the supramolecular hydrogels was first assessed using CMC-MPP⊂CB[8], with intermediate bonding affinity and crosslink dynamics of the motifs studied here, as a model hydrogel (***Fig 3a***) in comparison to supramolecular hydrogel samples subjected to either directional freeze-casting only or salting-out only. The combination of directional freeze-casting and salting-out led to a significant increase in Young's modulus (66 kPa) relative to either directional freeze-casting only (10 kPa) or salting out alone (35 kPa). Similarly, the hydrogel toughness (0-70% strain) following the combined processing steps (38.0 kJ/m^3) was also significantly greater than that for either directional freeze-casting (10.3 kJ/m^3) or salting-out (13.9 kJ/m^3) alone. Thus, the combined use of both directional freeze-casting and salting-out steps following hydrogel formation led to a synergistic effect on the compressive mechanical properties.

Next, the compressive mechanical behavior of the different guest-bearing hydrogels prepared by directional freeze-casting and salting-out were studied. Compressive properties were of specific interest here given a recent report that showed the emergence of high toughness under compression in networks crosslinked by heteroternary CB[8]–guest interactions having very slow exchange dynamics.[24] Compression was applied parallel to the direction of freeze-casting, corresponding to the dimension of toughening achieved when directional freeze-casting and salting-out are coupled.[7] CMC-PP⊂CB[8] exhibited the highest Young's modulus (122 ± 11 kPa) and toughness (83.7 ± 13.5 kJ/m^3), followed by CMC-MPP⊂CB[8] and CMC-CPP⊂CB[8] (***Fig 3b,***

Table 2: Results from compressive mechanical testing on the different CMC-Guest⊂CB[8] supramolecular hydrogels prepared at 5% (w/v) with toughness and Young's modulus (E) and toughness (U_t) were measured under uniaxial compression at 0-10% and 0-70% strain, respectively. Hysteretic energy dissipation (U_d) was measured under cyclic uniaxial compression to 60% strain on the 1st and 5th loading cycle. The mean ± standard deviation is reported from multiple sample replicates (n = *3/polymer*)

Polymer	E (kPa)	U_t (kJ m^{-3})	U_d, 1st Cycle (kJ m^{-3})	U_d, 5th Cycle (kJ m^{-3})
CMC-PP	122 ± 11	83.7 ± 13.5	25.1 ± 4.7	5.5± 0.8
CMC-MPP	60 ± 7	33.9 ± 3.8	10.1 ± 3.7	3.2 ± 1.0
CMC-CPP	45 ± 13	23.1 ± 8.5	9.7 ± 1.6	2.8 ± 0.2
CMC-BP	11 ± 4	4.1 ± 2.5	2.3 ± 0.8	0.8 ± 0.4
CMC-BM *(supra)*	33 ± 10	19.4 ± 9.9	6.0 ± 08	2.0 ± 0.6

Table 2). By comparison, CMC-BP⊂CB[8] yielded the lowest Young's modulus (11 ± 4 kPa) and toughness (4.1 ± 2.5 kJ/m^3). Importantly, this order corresponded to the ranking of affinities for the different CB[8]–guest interactions, pointing to a molecular scale origin of bulk hydrogel mechanical properties. Notably, although CMC-PP⊂CB[8] was the toughest hydrogel, the ultimate strain was below 70% and it exhibited visible cracks after compression tests (***Fig 3c***). Conversely, other hydrogels exhibited no signs of failure prior to reaching 75% strain. The Young's modulus for these hydrogels was of the same order as that shown for related work using heteroternary CB[8]–guest crosslinking, wherein networks prepared at roughly 20 wt% (2 M monomers in the polymerization mixture) had a Young's modulus in the range of 55-243 kPa, depending on the displacement rate of compression.[24] Accordingly, these 5 wt% CMC hydrogels compare reasonably on this measure of mechanical properties.

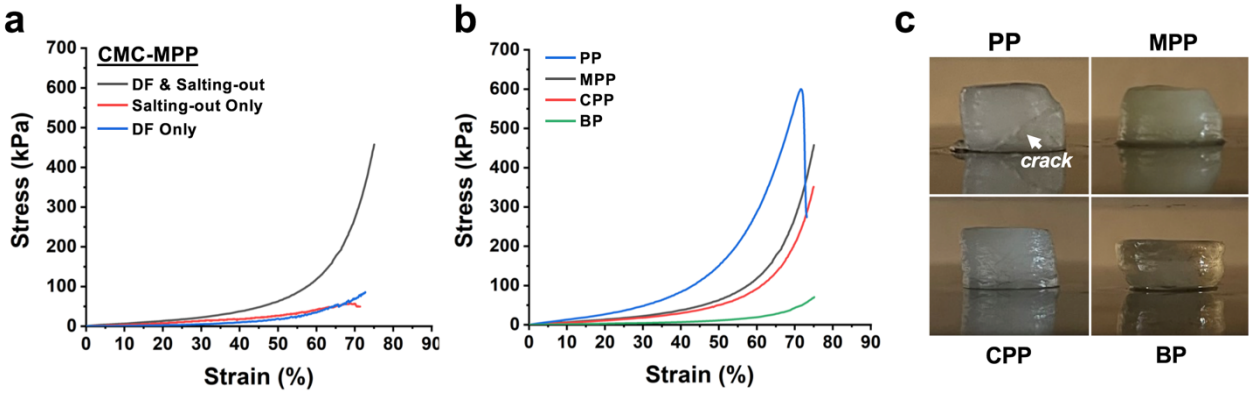

Figure 3: Compressive mechanical behavior of CMC-Guest⊂CB[8] supramolecular hydrogels prepared in DI water from guest-modified 90 kDa CMC at 5% (w/v). (**a**) Representative stress-strain curves for hydrogels processed by both directional freeze-casting (DF) and salting-out, compared to each step alone. (**b**) Representative stress-strain curves showing the effect of guest chemistry selection for hydrogels processed by directional freeze-casting and salting-out, with (**c**) representative images of samples after testing. Mechanical properties measured for each guest chemistry are reported in Table 2.

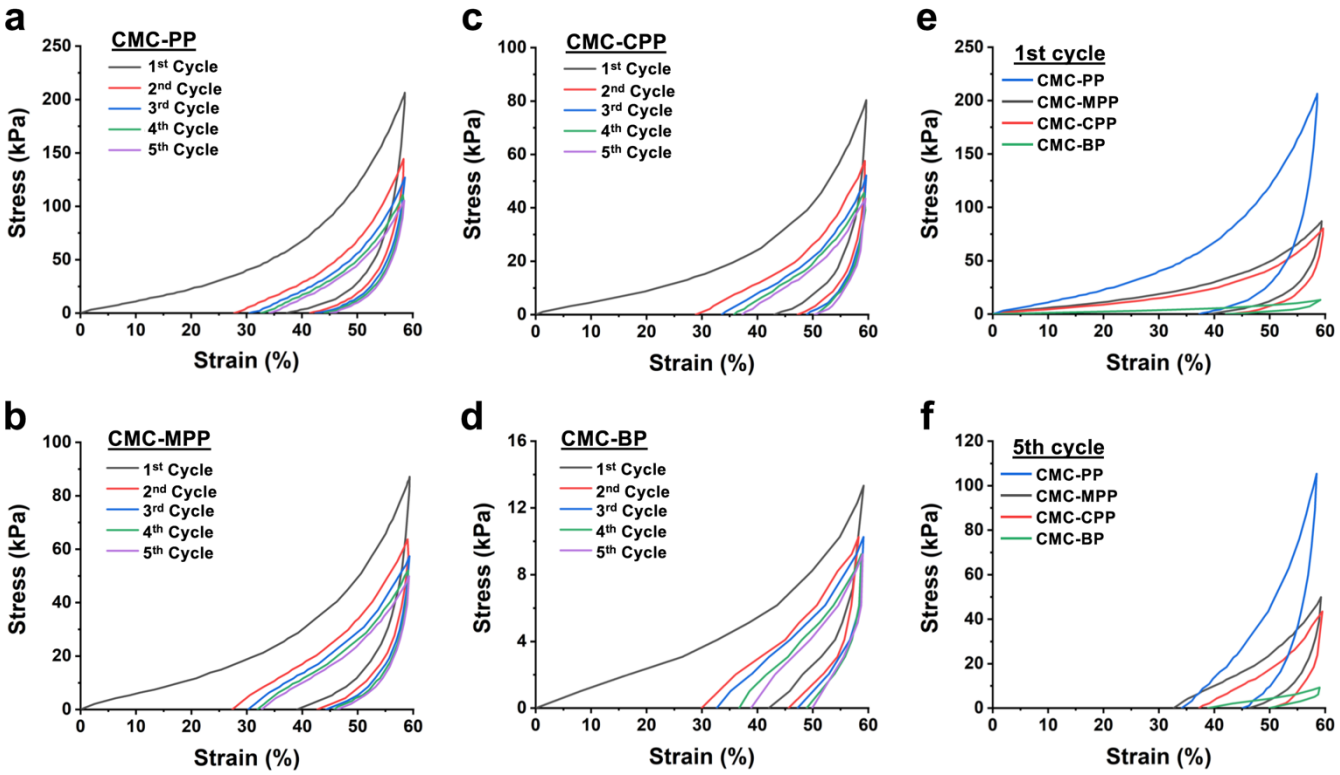

Figure 4: Compressive mechanical properties CMC-Guest⊂CB[8] supramolecular hydrogels prepared in DI water from guest-modified 90 kDa CMC at 5% (w/v) in all cases and cycled to 60% strain five times, comparing stress-strain behavior for guest chemistries of (**a**) CMC-PP, (**b**) CMC-MPP, (**c**) CMC-CPP, and (**d**) CMC-BP over each cycle. The different guest chemistries were also compared on the (**e**) first and (**f**) fifth cycle.

The recovery of CMC-guest⊂CB[8] hydrogels was next investigated under cyclic uniaxial compression for five loading cycles. A representative cyclic experiment is shown (***Movie S3***). The different guest-bearing hydrogels all exhibited maximal energy dissipation in the first cycle, followed by progressively decreased energy dissipation in the second through fifth cycles (***Fig 4a-d***). The loading and unloading curves were compared across the four different guest-modified hydrogels for the first (***Fig 4e***) and fifth (***Fig 4f***) cycles. Consistent with static compression tests, the energy dissipation for CMC-PP⊂CB[8] hydrogels was also the highest for both the first (25.1 ± 4.7 kJ/m^3) and fifth (5.5 ± 0.8 kJ/m^3) cycles (***Table 2***). The CMC-MPP⊂CB[8] and CMC-CPP⊂CB[8] hydrogels had similar energy dissipation, with both being significantly higher than CMC-BP⊂CB[8] hydrogels. These results followed the same trends evident in the affinity of each complex from ITC measurements (***Table 1***), as well as the static compressive mechanical properties of the hydrogels (***Table 2***). Moreover, these findings lend further support to the "*strong means slow*" principle which has previously demonstrated control over the bulk mechanical properties by tuning the dynamics of supramolecular crosslink exchange.[16] Prior work exploring slowly dynamic CB[8]–guest crosslinking interactions in polymer networks of ~20-56 wt% showed limited change in mechanical properties under cyclic compression.[24] The CMC hydrogels here were prepared at a lower polymer fraction (5 wt%) from comparatively much more dynamic and much less cooperative interactions than this prior work, and do show a progressive reduction in mechanical properties upon cyclic compression. Yet the underlying principles relating supramolecular affinity and its concomitant dynamics to mechanical properties hold for this more dynamic class of supramolecular materials in the trends observed here.

These studies demonstrate the toughening of supramolecular hydrogels arising through a combination of directional freeze-casting and salting-out. Interestingly, binding affinity and concomitant crosslink exchange dynamics of CB[8]–guest ternary complexes plays a crucial role in directing the mechanical properties of these hydrogels. Higher binding affinity leads to hydrogels with lower crosslink exchange dynamics when measured by oscillatory rheology, as expected,[19] as well as a higher Young's modulus and toughness under compressive loading. At the same time, the use of high-affinity interactions (e.g., PP) results in cracks under high compressive strains. This finding emphasizes the importance of tailoring the affinity and dynamics of supramolecular recognition of guest molecules to achieve a balance between mechanical strength and resilience of the resulting hydrogel, as appropriate for the desired application.

Supramolecular vs. Covalent Hydrogels. To study the effect of supramolecular crosslinking on the toughening effects obtained through directional freeze-casting and salting-out, a Brooker's merocyanine (BM) guest with similar structure to MPP was introduced onto CMC for supramolecular hydrogel formation. CB[8] catalyzes [2+2] photodimerization of BM, enabling the dynamic supramolecular motif to be converted into a static covalent crosslink upon the application of UV light.[22] The K_{eq} of BM-Ac in forming a homoternary supramolecular complex with CB[8] was measured using ITC (1.4 x 10^{13} M^{-1}), and thus was of the same order as that for MPP-Ac (***Table 1***). Accordingly, the intention of using the BM guest as an externally modulatable supramolecular crosslinking motif with CB[8] binding comparable to MPP was supported by molecular-scale characterization of the complex. The mechanical properties of supramolecular CMC-BM⊂CB[8] hydrogels were also comparable to CMC-MPP⊂CB[8] by rheology and compression testing. Specifically, the hydrogels had slow dynamics and frequency-dependent G' behavior (***Fig S28***), along with a Young's modulus during compression of similar order (33 ± 10 kPa, ***Fig 5a and Table 2***), without signs of cracking or failure up to 70% strain. Under cyclic compression, the supramolecular CMC-BM⊂CB[8] hydrogel also exhibited maximal energy dissipation during the first cycle, which was reduced to approximately one-third by the fifth cycle (***Fig 5b and Table 2***).

Dynamic character was lost upon UV-induced crosslinking of CMC-BM⊂CB[8] hydrogels, as evidenced by frequency-independent G' behavior in oscillatory rheology (***Fig S28***). This is consistent with previous results from hydrogels crosslinked with BM motifs upon UV-induced [2+2] photodimerization.[22] Under compression, the Young's modulus of the covalent hydrogel (35 kPa) was similar to that of the supramolecular CMC-BM⊂CB[8] hydrogel, but cracks formed at strains below 50% (***Fig 5a***). The self-healing properties of covalent and supramolecular CMC-BM⊂CB[8] hydrogels were also compared; hydrogels were cut in half with the halves then placed in physical contact along the edges that were divided by the cut and maintained within a sealed vial at room temperature for 7 d before compression testing, in comparison to pristine hydrogels exposed to the same conditions without cutting (***Fig 5c***). The supramolecular CMC-BM⊂CB[8] hydrogel that was cut in half exhibited a stress-strain curve that was nearly identical to the pristine hydrogel up to a strain of approximately 60%. By comparison, the crosslinked CMC-BM⊂CB[8] that was cut in half did not self-heal and fractured immediately upon initiating compressive loading. Self-healing in the supramolecular hydrogel arises from dynamic rearrangement of supramolecular crosslinking to heal the defect over the 7 d healing period, a feature lost upon UV-induced conversion of the supramolecular BM_2⊂CB[8] to its static covalent form. It was previously shown that even among supramolecular hydrogels, crosslinking interactions with very slow rates of dynamic exchange fail to heal defects arising from cutting;[19] accordingly crosslinking in the supramolecular CMC-BM⊂CB[8] affords the requisite dynamics to facilitate healing.

The introduction of a BM guest, enabling subsequent conversion of the supramolecular CMC-BM⊂CB[8] hydrogel into a covalent hydrogel, offers specific insight into the importance of supramolecular crosslinking on hydrogel toughening in conjunction with directional freeze-casting and salting-out. Though the covalent hydrogel exhibits a similar Young's modulus as the supramolecular version, its mechanical strength and self-healing were compromised upon crosslink conversion. The improvement in self-healing character for the supramolecular hydrogels relative to their covalent counterparts is consistent with expectations. Furthermore, these findings challenge the traditional notion that covalent hydrogels are mechanically stronger than supramolecular hydrogels, instead suggesting a crucial role

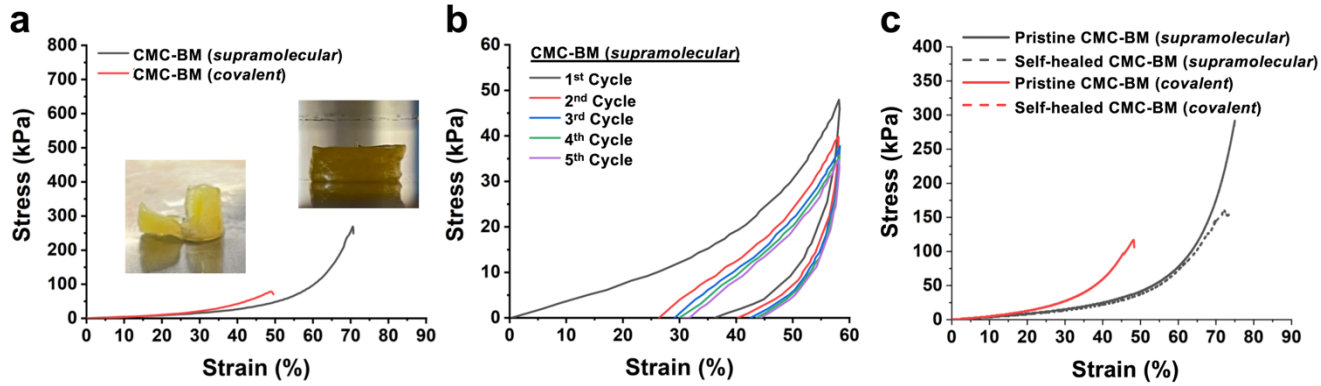

Figure 5: Compressive mechanical behavior CMC-BM⊂CB[8] supramolecular hydrogels as well as the UV-induced covalent crosslinked version of this same chemistry, prepared in DI water from guest-modified 90 kDa CMC at 5% (w/v), (**a**) comparing stress-strain curves for the supramolecular vs. covalent crosslinking chemistry. (**b**) Stress-strain curves for CMC-BM⊂CB[8] supramolecular hydrogels loaded to 60% strain for five cycles. (**c**) CMC-BM⊂CB[8] supramolecular hydrogels and UV-induced covalent crosslinked hydrogels that were prepared and processed identically. Samples were either stored for 7 d (pristine) or cut in half and then placed in physical contact for 7 d (self-healed) prior to loading in compression.

for dynamic supramolecular crosslinks in preparing tough hydrogels in conjunction with directional freeze-casting and salting-out that are resistant to critical failure and afford self-healing characteristics.

Conclusions

This current study emphasizes the importance of combining crosslinking *via* supramolecular recognition alongside processing steps of directional freeze-casting and salting-out in order to develop mechanically tough and self-healing supramolecular hydrogels. Using these processing steps to achieve hierarchically organized materials, the underlying molecular-scale crosslink dynamics serve to govern the bulk mechanical outcomes. This work offers further evidence of supramolecular networks with enhanced mechanical properties that arise from slowing molecular scale dynamics of crosslinking exchange in the network, aligning with findings demonstrated in related systems.[16,24] Moreover, using the BM guest chemistry here enables a supramolecular network to be converted *in situ* into an analogous covalent network, offering direct evidence for the importance of supramolecular dynamics in preparing hydrogel networks with enhanced toughness and self-healing ability. The present findings thus highlight the critical role of tailoring the binding affinity of guest molecules and the advantages of supramolecular crosslinking in achieving tunable mechanical properties and self-healing, offering strategy to prepare hydrogels aligning with the needs of a specific application. Future research should therefore focus on optimizing the molecular-scale dynamics of crosslinking interactions and integrating these with material design and fabrication techniques to develop supramolecular hydrogel materials with unique and customizable properties and enhanced performance controlled across length scales, thereby empowering a wide range of applications.

Acknowledgements

MJW gratefully acknowledges funding support for this work from a National Science Foundation CAREER award (BMAT, 1944875), and a 3M Young Investigator Award. We are also grateful to the NDEnergy Materials Characterization Facility for use of the rheometer. TOC graphic and Figure 1 were prepared using BioRender.com.

Keywords: biomaterials • rheology • hydrogels • Bio-Inspired Materials

References:

[1] X. Yuan, Z. Zhu, P. Xia, Z. Wang, X. Zhao, X. Jiang, T. Wang, Q. Gao, J. Xu, D. Shan, B. Guo, Q. Yao, Y. He, *Adv. Sci.* **2023**, *10*, e2301665.

[2] M. Sun, H. Li, Y. Hou, N. Huang, X. Xia, H. Zhu, Q. Xu, Y. Lin, L. Xu, *Sci Adv* **2023**, *9*, eade6973.

[3] A. Pena-Francesch, H. Jung, M. C. Demirel, M. Sitti, *Nat. Mater.* **2020**, *19*, 1230.

[4] C.-L. He, F.-C. Liang, L. Veeramuthu, C.-J. Cho, J.-S. Benas, Y.-R. Tzeng, Y.-L. Tseng, W.-C. Chen, A. Rwei, C.-C. Kuo, *Adv. Sci.* **2021**, *8*, e2102275.

[5] S. Lin, J. Liu, X. Liu, X. Zhao, *Proc. Natl. Acad. Sci. U. S. A.* **2019**, *116*, 10244.

[6] T. Matsuda, R. Kawakami, R. Namba, T. Nakajima, J. P. Gong, *Science* **2019**, *363*, 504.

[7] M. Hua, S. Wu, Y. Ma, Y. Zhao, Z. Chen, I. Frenkel, J. Strzalka, H. Zhou, X. Zhu, X. He, *Nature* **2021**, *590*, 594.

[8] M.-A. Shahbazi, M. Ghalkhani, H. Maleki, *Adv. Eng. Mater.* **2020**, *22*, 2000033.

[9] H. Zhang, I. Hussain, M. Brust, M. F. Butler, S. P. Rannard, A. I. Cooper, *Nat. Mater.* **2005**, *4*, 787.

[10] X. Guo, X. Dong, G. Zou, H. Gao, W. Zhai, *Sci Adv* **2023**, *9*, eadf7075.

[11] A. M. Hyde, S. L. Zultanski, J. H. Waldman, Y.-L. Zhong, M. Shevlin, F. Peng, *Org. Process Res. Dev.* **2017**, *21*, 1355.

[12] R. Sadeghi, F. Jahani, *J. Phys. Chem. B* **2012**, *116*, 5234.

[13] Z. Wang, X. Zheng, T. Ouchi, T. B. Kouznetsova, H. K. Beech, S. Av-Ron, T. Matsuda, B. H. Bowser, S. Wang, J. A. Johnson, J. A. Kalow, B. D. Olsen, J. P. Gong, M. Rubinstein, S. L. Craig, *Science* **2021**, *374*, 193.

[14] M. Wang, P. Zhang, M. Shamsi, J. L. Thelen, W. Qian, V. K. Truong, J. Ma, J. Hu, M. D. Dickey, *Nat. Mater.* **2022**, *21*, 359.

[15] M. J. Webber, M. W. Tibbitt, *Nature Reviews Materials* **2022**, *7*, 541.

[16] Y. Li, C. Zhu, Y. Dong, D. Liu, *Polymer* **2020**, *210*, 122993.

[17] M. J. Webber, E. A. Appel, E. W. Meijer, R. Langer, *Nat. Mater.* **2016**, *15*, 13.

[18] S. M. Mantooth, B. G. Munoz-Robles, M. J. Webber, *Macromol. Biosci.* **2019**, *19*, e1800281.

[19] L. Zou, A. S. Braegelman, M. J. Webber, *ACS Appl. Mater. Interfaces* **2019**, *11*, 5695.

[20] S. J. Barrow, S. Kasera, M. J. Rowland, J. del Barrio, O. A. Scherman, *Chemical Reviews* **2015**, *115*, 12320.

[21] H.-J. Kim, J. Heo, W. S. Jeon, E. Lee, J. Kim, S. Sakamoto, K. Yamaguchi, K. Kim, *Angew. Chem. Int. Ed Engl.* **2001**, *40*, 1526.

[22] L. Zou, M. J. Webber, *Chem. Commun.* **2019**, *55*, 9931.

[23] E. A. Appel, F. Biedermann, U. Rauwald, S. T. Jones, J. M. Zayed, O. A. Scherman, *J. Am. Chem. Soc.* **2010**, *132*, 14251.

[24] Z. Huang, X. Chen, S. J. K. O'Neill, G. Wu, D. J. Whitaker, J. Li, J. A. McCune, O. A. Scherman, *Nat. Mater.* **2022**, *21*, 103.

[25] J. Xu, X. Zhu, J. Zhao, G. Ling, P. Zhang, *Adv. Colloid Interface Sci.* **2023**, *321*, 103000.

[26] Y. Zhang, T.-Y. Zhou, K.-D. Zhang, J.-L. Dai, Y.-Y. Zhu, X. Zhao, *Chem. Asian J.* **2014**, *9*, 1530.

[27] L. Zou, C. J. Addonizio, B. Su, M. J. Sis, A. S. Braegelman, D. Liu, M. J. Webber, *Biomacromolecules* **2021**, *22*, 171.

[28] H. Zhao, G. Piszczek, P. Schuck, *Methods* **2015**, *76*, 137.

[29] Z. Huang, K. Qin, G. Deng, G. Wu, Y. Bai, J.-F. Xu, Z. Wang, Z. Yu, O. A. Scherman, X. Zhang, *Langmuir* **2016**, *32*, 12352.

[30] E. Cavatorta, P. Jonkheijm, J. Huskens, *Chemistry* **2017**, *23*, 4046.

[31] Y. Xu, L. Li, P. Zheng, Y. C. Lam, X. Hu, *Langmuir* **2004**, *20*, 6134.